Received: 21 July 2020 | Revised: 5 October 2020 | Accepted: 31 October 2020

DOI: 10.1002/ardp.202000258

FULL PAPER

ARCH PHARM DPhG
Archiv der Pharmazie

Novel *N*-benzylpiperidine derivatives of 5-arylisoxazole-3-carboxamides as anti-Alzheimer's agents

Mina Saeedi[1,2] | Peyman Felegari[3] | Aida Iraji[4] | Roshanak Hariri[3] | Arezoo Rastegari[2] | S. Sara Mirfazli[5] | Najmeh Edraki[4] | Omidreza Firuzi[4] | Mohammad Mahdavi[6] | Tahmineh Akbarzadeh[2,3]

[1]Medicinal Plants Research Center, Faculty of Pharmacy, Tehran University of Medical Sciences, Tehran, Iran

[2]Persian Medicine and Pharmacy Research Center, Tehran University of Medical Sciences, Tehran, Iran

[3]Department of Medicinal Chemistry, Faculty of Pharmacy, Tehran University of Medical Sciences, Tehran, Iran

[4]Medicinal and Natural Products Chemistry Research Center, Shiraz University of Medical Sciences, Shiraz, Iran

[5]Department of Medicinal Chemistry, School of Pharmacy-International Campus, Iran University of Medical Sciences, Tehran, Iran

[6]Endocrinology and Metabolism Research Center, Endocrinology and Metabolism Clinical Sciences Institute, Tehran University of Medical Sciences, Tehran, Iran

Correspondence
Tahmineh Akbarzadeh, Department of Medicinal Chemistry, Faculty of Pharmacy, Tehran University of Medical Sciences, Tehran, Iran.
Email: akbarzad@tums.ac.ir

Abstract

The complex pathophysiology of Alzheimer's disease (AD) has prompted researchers to develop multitarget-directed molecules to find an effective therapy against the disease. In this context, a novel series of *N*-(1-benzylpiperidin-4-yl)-5-arylisoxazole-3-carboxamide derivatives were designed, synthesized, and evaluated against acetylcholinesterase (AChE) and butyrylcholinesterase (BuChE). In vitro biological evaluation demonstrated that compound **4e** was the best AChE (IC_{50} = 16.07 μM) and BuChE inhibitor (IC_{50} = 15.16 μM). A kinetic study of **4e** was also conducted, which presented a mixed-type inhibition for both enzymes. Molecular docking studies revealed that compound **4e** fitted well into the active sites of AChE and BuChE, forming stable and strong interactions with key residues Glu199, Trp84, Asp72, Tyr121, and Phe288 in AChE and His438, Trp82, Ala328, Tyr332, Phe329, Thr120, and Pro285 in BuChE. Besides, the inhibition of BACE1 by **4e** and the biometal chelation activity of **4e** were measured. The neuroprotective assessment revealed that **4e** exhibited 23.2% protection at 50 μM toward amyloid-beta-induced PC12 neuronal cells. Overall, this study exhibited that compound **4e** was a promising compound targeting multiple factors associated with AD.

KEYWORDS

Alzheimer's disease, BACE1, cholinesterase, isoxazoles, multitarget compound, neuroprotection

1 | INTRODUCTION

Alzheimer's disease (AD) is a progressive neurodegenerative disease and one of the leading causes of morbidity and mortality in elderly people with a continuous deterioration of cognition, memory, aphasia, behavior, and personality.[1] AD is a complex multifactorial disease with many contributing factors. The physiopathology of the disease is characterized by the formation of amyloid-beta (Aβ) senile plaques as extracellular deposits and neurofibrillary tangles as intracellular ones. The proteolytic cleavage of amyloid precursor protein (APP) by β-site APP-cleaving enzyme 1 (BACE1) and the γ-secretase complex lead to the formation of Aβ plaques. The extracellular deposition of Aβ triggers a cascade of pathological events including inflammation, mitochondrial dysfunctions, oxidative stress, and finally cell death. There is growing evidence that BACE1 inhibitors could lessen APP cleavage and effectively reduce Aβ with low synaptotoxicity.[2]

On the basis of different paths to the pathogenesis of AD, dysfunction and lack of neurotransmissions, especially acetylcholine

This paper is dedicated to the memory of our unique Chemistry and Medicinal Chemistry teacher, Professor Abbas Shafiee (1937–2016).

(ACh), deteriorate brain networks, which in turn results in loss of synapses. Low amounts of ACh are mainly attributable to the enhanced degradation rate of ACh by two known cholinesterase (ChE) enzymes known as acetylcholinesterase (AChE) and butyrylcholinesterase (BuChE).[3] Considering the high expression of AChE at the early stage of AD, acetylcholinesterase inhibitors (AChEIs) are the first line of therapy in the primary-to-moderate stage of AD such as rivastigmine, donepezil, and galantamine. However, due to the increasing amount of BuChE at the late stage of AD, butyrylcholinesterase inhibitors (BuChEIs) could be an ideal candidate for moderate-to-severe AD.[4]

Inflammation is another basic mechanism of AD pathophysiology in addition to Aβ.[5] Prolonged inflammation becomes chronic inflammation, which can cause detrimental effects on brain functions due to excessive or persistent release of toxic factors.[6] It has been demonstrated that excessive production of Aβ activates chemokine and cytokines, releases the proinflammatory agents, and promotes inflammation further.[7]

Also, there is a large amount of evidence confirming the involvement of biometals in AD pathogenesis. Metal ion dyshomeostasis and metal-induced Aβ aggregation are considered as other biochemical factors related to AD.[8] In this regard, metal interactions with Aβ and tau influence their aggregation properties and neurotoxicity. Also, on the basis of Fenton reactions, the unregulated interactions of metal with molecular oxygen facilitate the generation of reactive species (reactive oxygen species and reactive nitrogen species), which results in increased levels of lipid peroxidation and oxidative damage to DNA and proteins.[9,10]

There is no fully effective cure for AD yet. Recent failures of several AD clinical trials confirmed the complicated and multifactorial nature of AD pathogenesis, which leads to irreversible neurodegeneration and neural network damage.[11]

In this regard, comprehensive pieces of evidence support the role of multitarget direct ligands (MTDLs) as possible therapeutic agents. In this case, simultaneous inhibition of AChE, BuChE, and BACE1 by *N*-(1-benzylpiperidin-4-yl)-5-arylisoxazole-3-carboxamides, combined with neuroprotective and biometal chelation activities, were considered.

2 | RESULTS AND DISCUSSION

2.1 | Structure-based design of benzylpiperidine-arylisoxazole-carboxamides

Donepezil (**A**; Figure 1) is known as a Food and Drug Administration-approved AChEI in which the benzylpiperidine tail interacts with the PAS residues of the AChE pocket and the 2,3-dihydroindenone moiety occupies the CAS pocket. Many of ChEIs typically mimic the structural feature of the benzylpiperidine tail. This is evidenced by the result of compound **B**, which exhibited potent AChE inhibition with an IC_{50} value of 21.85 μM and BuChE inhibition with an IC_{50} value of 76.78 μM. This compound also demonstrated 22% BACE1 inhibition at 50 μM.[12] We also recently reported ChEI (compound **C**; Figure 1) with an arylisoxazole structure containing a benzyl-pyridine tail.

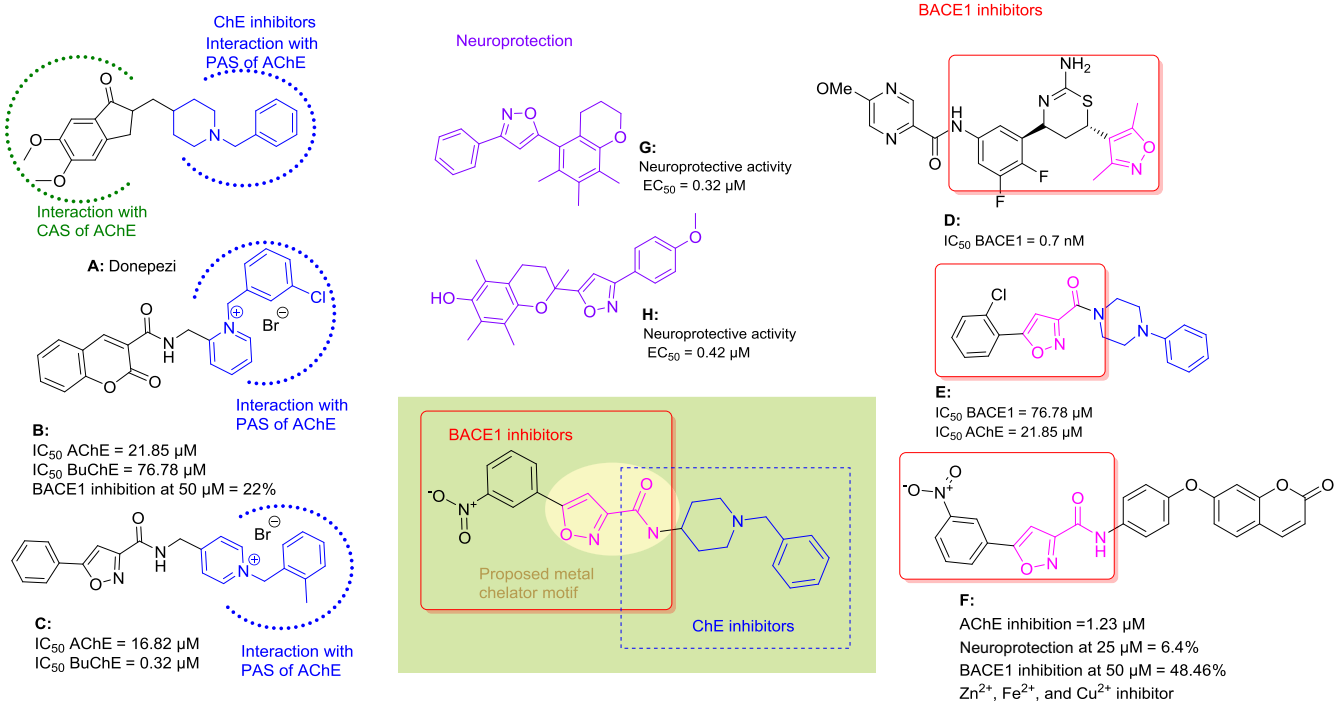

FIGURE 1 The design of novel *N*-benzylpiperidine derivatives of 5-arylisoxazole-3-carboxamides

This compound depicted a selective BuChEI activity (IC_{50} = 0.32 μM) with moderate AChE inhibition.[13]

Most of the potent BACE1 inhibitors are peptidic and pseudo-peptidic molecules with high similarity with the structure of APP as a substrate. One of the most efficient ones is OM99-2 with an IC_{50} value of 14.7 nM.[14] However, due to poor physicochemical and pharmaceutical properties, including insufficient oral bioavailability, short serum half-life, and low blood–brain barrier penetration, there is an ongoing interest to design small-molecule BACE1 inhibitors.[3] For the past few years, there have been many synthetic BACE1 inhibitors; among such compounds, there are limited examples of the isoxazole-3-carboxamides molecular skeleton as the core structure. Compound **D** (Figure 1) was developed according to the property and structure-based approach via incorporation of the dimethylisoxazole substitution into the aminothiazine carboxamide series as potent and selective BACE1 inhibitors.[15] From literature reports, it is also stated that the amide-arylisoxazole core is involved in BACE1 inhibition due to its key structural feature of heterocyclic compounds and the capability of forming hydrogen bonds with the BACE1 active site.[3] In this respect, aryl isoxazol-corporating phenylpiperazine (compound **E**) showed moderate BACE1 inhibitory activity (IC_{50} = 76.78 μM). Compound **E** also showed selectivity toward AChE, compared with BuChE.[16] We previously reported the discovery of a series of arylisoxazole-chromenone carboxamide derivatives (compound **F**) with general structure **F** with good BACE1 inhibitory potency.[17] Besides, the in vitro AChE inhibitory activity was highly dependent on the presence and position of nitro substituents. The greatest activity occurred when the nitro group was located at the 3-position, whereas 4- and 5-methoxy derivatives were inactive. Also, **F** depicted 84.9% neuroprotectivity at the concentration of 50 μM (Figure 1). Meanwhile, several isoxazole-containing motifs (**F**, **G**, **H**) were also reported to display neuroprotective, anti-inflammatory, and antioxidant activities.[18,19]

Consequently, a pharmacophoric hybridization strategy was adopted to design and synthesize new small MTDLs possessing arylisoxazole-carboxamide as a core skeleton. To improve ChE inhibitory potency, the benzylpiperidine moiety with ensured anti-ChE properties was incorporated into the isoxazole-3-carboxamides scaffold. On the basis of the demonstrated structure, it can be understood that the presence of the amide moiety played an important role in inducing appropriate ChE and BACE1 inhibitory activity. Besides, the mentioned scaffold seems to enhance anti-AD biological properties featured by BACE1 inhibitory, anti-inflammatory, metal chelation endeavors. The presence of a heterocyclic structure with the carboxamide linker may also amplify the metal chelation potential of the designed scaffold. The structural derivatization of target compounds mainly focused on the substitution of the arylisoxazole-3-carboxamides at various positions of the aryl ring.

2.2 | Chemistry

The synthesis of desired compounds **4** was achieved according to Scheme 1. The desired carboxylic acid derivatives **2** were prepared through a three-step reaction, as reported in our previous work.[17] Then, the reaction of compounds **2** and **3** in the presence of hydroxybenzotriazole (HOBT) and 1-ethyl-3-(3-dimethylaminopropyl) carbodiimide (EDCI) in dry acetonitrile at room temperature afforded the target compound **4**. The structure of all compounds was confirmed using nuclear magnetic resonance (NMR) and infrared (IR) spectroscopy, as well as elemental analysis. It should be noted that in the case of compounds **4a**, **4c**, **4g**, **4h**, and **4j**, the ^{13}C NMR spectra showed the presence of two isomers probably due to restricted C–N amide bond rotation. It is clear that the formation of rotamers is dependent on the electronic effects and steric hindrance of substituents on the aryl ring, as they can affect the C–N rotational barrier and planarity of the amide carbonyl group. It seems that the presence of the electron-withdrawing group (NO_2) led to a lower C–N rotational barrier. In the case of electron-donating groups and halogens, their steric effect and size as well as their positions on the aryl ring are very important. When the aromatic ring was unsubstituted (compound **4a**) or occupied by the small-size halogen (F) at *ortho* or *para* positions (compounds **4g** and **4h**), the formation of rotamers was confirmed by ^{13}C NMR, which can also be observed in the case of a medium-size halogen (Cl) at the *para* position (compound **4j**). However, a change of its position to *ortho* (compound **4i**) or increasing the number of Cl (compound **4k**) deplanarized the carbonyl group and stopped rotamerization. This can also be observed in compound **4l** with a large-size halogen (Br). Our results related to the electron-donating substituted derivatives (compounds **4**b-**4d**) revealed that the presence of those groups only at the *meta* position led to a higher C–N rotational barrier.

2.3 | Biology

2.3.1 | In vitro ChE inhibitory activities

All synthesized derivatives of compound **4** were evaluated for their biological activity against AChE and BuChE, whereas donepezil was

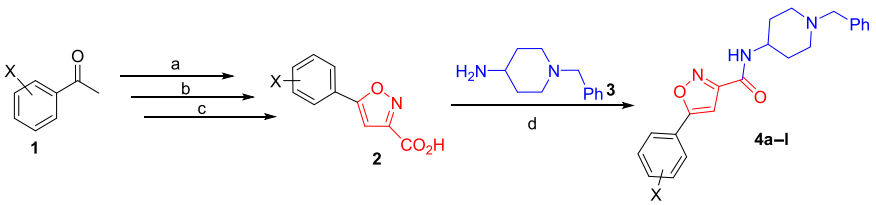

SCHEME 1 The synthesis of compound **4**. Reagents and conditions: (a) Diethyl oxalate, NaOEt/dry EtOH, 0°C-rt, 15 h; (b) $NH_2OH{\cdot}HCl$, EtOH, reflux, 3 h; (c) KOH, MeOH, reflux, 3 h; (d) HOBT, EDCI, dry CH_3CN, rt, 24–72 h

TABLE 1 Cholinesterase inhibitory activity of *N*-benzylpiperidine derivatives of 5-arylisoxazole-3-carboxamides **4a**–**l**[a]

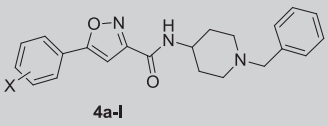

4a-l

Entry	Compound 4	X	AChEI [IC_{50} (μM)]	BuChEI [IC_{50} (μM)]	Selectivity[b]
1	**4a**	H	>100	53.29 ± 1.65	>0.5
2	**4b**	4-Me	>100	>100	–
3	**4c**	3-OMe	>100	47.46 ± 1.87	>0.5
4	**4d**	3,4-$(OMe)_2$	45.01 ± 0.92	>100	>2.2
5	**4e**	3-NO_2	16.07 ± 0.07	15.16 ± 0.22	>0.9
6	**4f**	4-NO_2	23.63 ± 0.38	>100	>4.2
7	**4g**	2-F	47.22 ± 1.16	26.46 ± 0.39	>0.6
8	**4h**	4-F	>100	>100	–
9	**4i**	2-Cl	>100	50.88 ± 0.21	>0.5
10	**4j**	4-Cl	>100	>100	–
11	**4k**	2,4-Cl_2	39.83 ± 0.38	>100	>2.5
12	**4l**	4-Br	>100	>100	–
Donepezil			0.28 ± 0.002	8.06 ± 0.38	

Abbreviations: AChE, acetylcholinesterase; BuChE, butyrylcholinesterase.

[a]Data are represented in terms of mean ± *SD*.

[b]Selectivity for AChE = IC_{50} (BuChE)/IC_{50} (AChE).

used as a positive control. The results are summarized in Table 1, and the SAR of these arylisoxazole derivatives was investigated. In the series hybrids, compound **4e** bearing *meta*-nitroaryl was the most potent ChEI, whereas the highest selective inhibitor of BuChE was compound **4c** with an IC_{50} value of 47.46 μM. Furthermore, **4f** (X = *para*-nitro) was regarded as the most selective AChEI.

In the case of AChE, the following conclusions can be drawn:

- The unsubstituted compound **4a** displayed no AChE inhibitory property in the whole range of concentrations studied.
- Compounds **4b** and **4c** bearing the electron-donating group, including methyl and methoxy, on the arylisoxazole ring were inactive; however, compound **4d** containing 3,4-diOMe showed a moderate inhibitory activity with an IC_{50} value of 45.01 μM.
- The presence of halogen atoms at the *para* position of arylisoxazole moiety led to a lack of activity. However, in the case of fluorine, switching X from *para* (**4h**) to *ortho* (**4g**) led to the active compound **4g** (IC_{50} = 47.22 μM). For the series of halogen-substituted derivatives, the highest activities were observed when the substitution occurred at the multiposition of the arylisoxazole. This is obvious in compound **4k** bearing 2,4-diCl at X position with an IC_{50} value of 39.83 μM.
- Furthermore, compounds **4e** (X = 3-NO_2, IC_{50} = 16.07 μM) and **4f** (X = 4-NO_2, IC_{50} = 23.63 μM) exhibited the best AChE inhibitory properties. Our results are in accordance with previously published data confirming the promising role of 3-nitroarylisoxazole in the AChE inhibitory activity.[17]

The results of anti-BuChE inhibitory activity indicated the following points:

- The absence of substituents on the phenylisoxazole pendant (compound **4a**) afforded a moderate inhibitory activity (IC_{50} = 53.29 μM).
- A comparison of the potency of the six halogenated arylisoxazole-benzylpiperidine hybrids (**4h**–**l**) revealed that the activity was affected by their positions. More specifically, the *para*-substituted derivatives (**4h**: X = 4-F, **4j**: X = 4-Cl, and **4l**: X = 4-Br) did not afford any BuChE inhibitory activity. Yet, changing the position of the halogen atom from *para* to *ortho* position of the aryl ring (**4g** vs. **4h** and **4i** vs. **4h**) provided a better BuChE inhibitory activity. This is obvious from the IC_{50} values for compounds **4g** and **4i** with 26.46 and 50.88 μM, respectively.
- From the screening data, the best BuChE inhibitory potency belongs to **4e** (X = 3-NO_2) with an IC_{50} value of 15.16 while changing *meta* to *para* (compound **4f**, X = 4-NO_2, IC_{50} > 100 μM) deleted BuChE inhibitory activity.

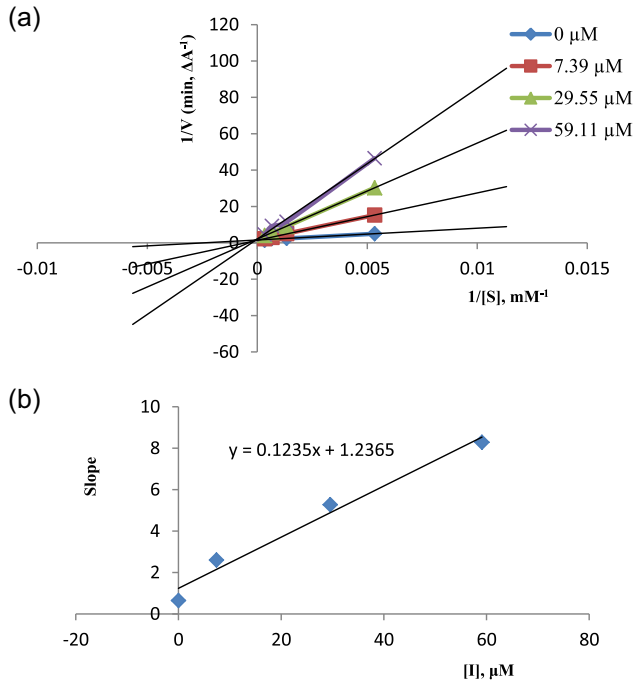

FIGURE 2 A kinetic study of inhibitor **4e** against acetylcholinesterase. The Lineweaver–Burk plot (a) and double-reciprocal Lineweaver–Burk plot (b) are shown

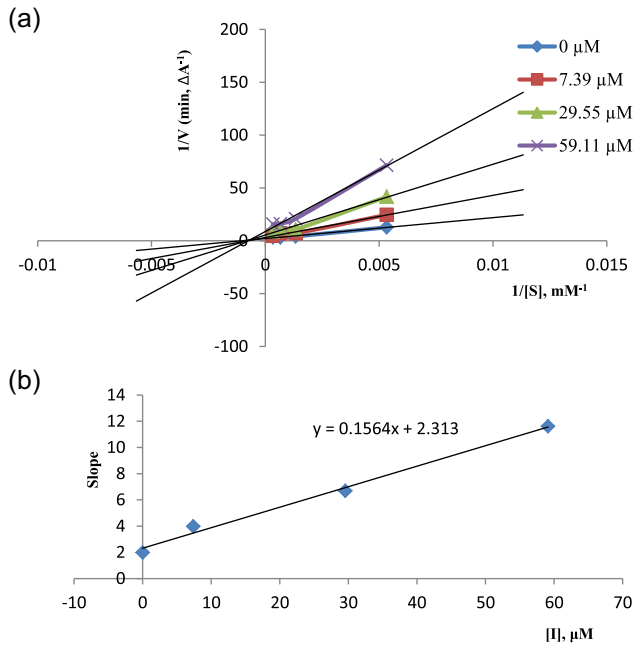

FIGURE 3 A kinetic study of inhibitor **4e** against butyrylcholinesterase. The Lineweaver–Burk plot (a) and double-reciprocal Lineweaver–Burk plot (b) are shown

- A comparison of inhibitory capabilities of **4a–l** showed that compound **4c** bearing 3-OMe with an IC_{50} value of 47.46 was the most selective BuChEI. The results indicated that the introduction of an extra methoxy group on the arylisoxazole moiety removed BuChE inhibitory activity (**4d**; X = 3,4-diOMe, IC_{50} > 100 µM).

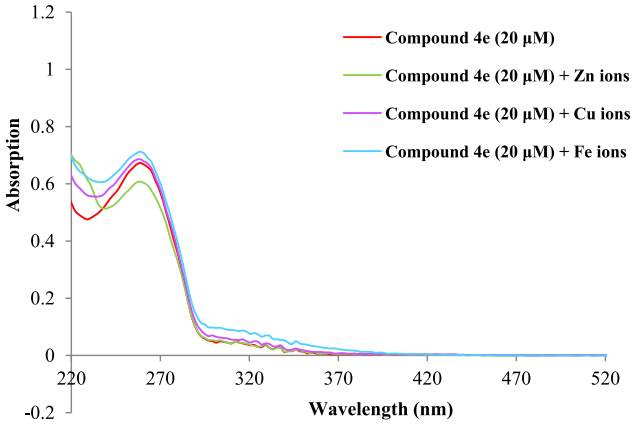

FIGURE 4 The absorbance change of compound **4e** alone and in the presence of Zn^{2+}, Fe^{2+}, and Cu^{2+} ions at a wavelength range of 200–600 nm

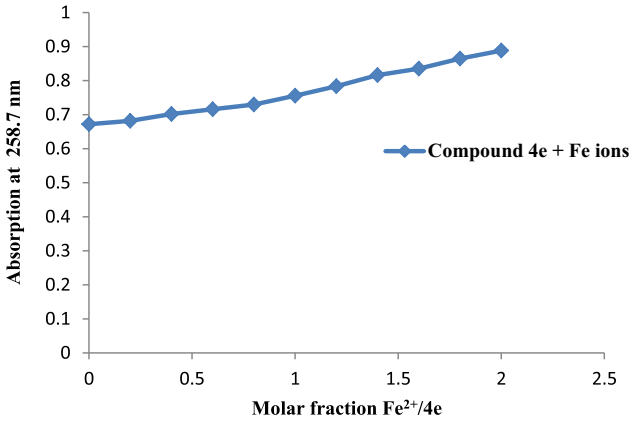

FIGURE 5 Absorption at 258.7 nm (λ_{max}), depending on the mole fraction of Cu^{2+} toward compound **4e**

2.3.2 | Kinetic studies

Kinetic studies were conducted to examine the mechanism of inhibition by compound **4e** toward AChE and BuChE, respectively. A graphical analysis of the reciprocal Lineweaver–Burk plot related to compound **4e** described a mixed-type inhibition pattern against both AChE and BuChE (Figures 2 and 3), indicating that **4e** can bind to both enzymes, even if it is already bound to the substrate. In addition, the K_i values were calculated using the secondary plot as 10.0 and 6.0 µM for AChE and BuChE inhibition (Figures 2b and 3b).

2.3.3 | BACE1 enzymatic assay

To further analyze the effect of anti-AD activities, compound **4e** with potent inhibitory activity against ChE was selected for the BACE1

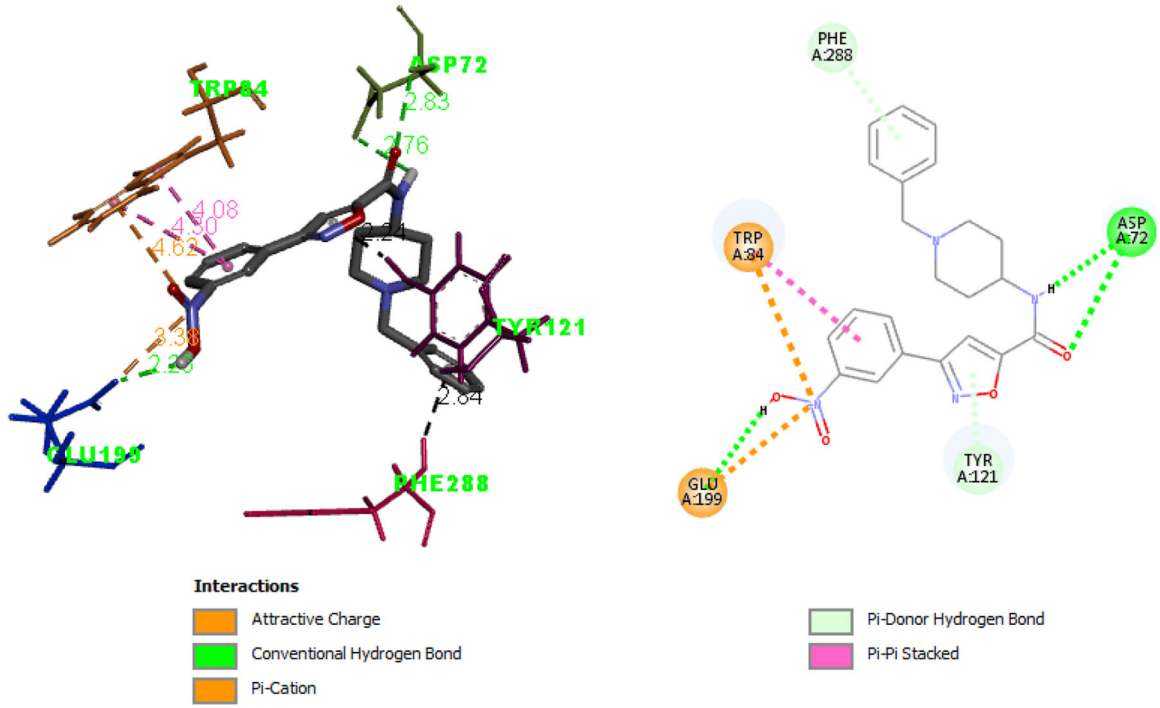

FIGURE 6 Docking of compound **4e** into the binding pocket of the 1EVE

inhibition assay. In this assay, OM99-2 (Glu-Val-Asn-Leu-Ala-Ala-Glu-Phe) was used as a reference compound with an IC_{50} value of 14.7 ± 2.8 nM. It was found that compound **4e** showed 10.9% and 24.3% inhibition toward BACE1 at the concentrations of 10 and 50 μM, respectively.

2.3.4 | Neuroprotection effect against Aβ-induced damage

Neurodegeneration and neuroinflammation have been known as two of the main complications of AD.[20] Hence, it was necessary to assess the neuroprotective properties of the potent candidate. As a result, compound **4e** was evaluated on PC12 neuronal cell-induced Aβ damage using the 3-(4,5-dimethylthiazol-2-yl)-2,5-diphenyltetrazolium bromide (MTT) viability assay, and the mentioned compound depicted 23.2% protection at 50 μM. Caffeic acid as a positive control protected the PC12 cells with an IC_{50} value of 75.8 ± 11.3 μM.

2.3.5 | Metal chelating activity

Compound **4e** was tested for its metal chelating ability toward Fe^{2+}, Cu^{2+}, and Zn^{2+} ions (Figure 4). The ultraviolet spectrum of methanolic solution (final concentration of 20 μM) of that compound showed a characteristic absorption peak at 258.7 nm. After the interaction of compound **4e** with metal ions for 30 min, as shown in Figure 4, no significant red and blue shifts were observed, and the change of intensity after interaction of compound **4e** and the corresponding metal ions indicated the formation of **4e**–metal complex. However, the results depicted that the chelation between compound **4e** and Cu^{2+} ions was not as optimally effective as that of Zn^{2+} and Fe^{2+} ions.

The stoichiometry of complex **4e**–Fe^{2+} was also studied (Figure 5). The concentration of the test compound **4e** was 20 μM and the final concentration of Fe^{2+} ranged from 0 to 40 μM, with 4-μM intervals at 258.7 nm. The plot was obtained by the corresponding absorption against the mole fraction of Fe^{2+} toward ligand (compound **4e**). According to the plot, the complexation ratio of 1:1 of **4e**–Fe^{2+} can be seen at the fracture point of the plot with the mole fraction of 0.8.

2.4 | Docking study

AutoDock software was used for the protein–ligand interaction study. The molecular modeling simulation of compound **4e** was carried out in 1EVE, 1P0P, and 2QP8. The range of minimized affinity values of the poses of the docked ligand into the AChE enzyme (1EVE) is −12.1 to −10.5 kcal/mol. The interactions of the best-docked confirmation of new ligand with the active site residues of 1EVE are depicted in Figure 6.

The analysis of binding interactions illustrated that the nitro substituent of the active molecule displayed substantial binding within the active site through conventional hydrogen bond and π stacking interactions via Glu199 and Trp84, whereas at the opposite site, the carbonyl group and NH of amide linker formed H-bonding

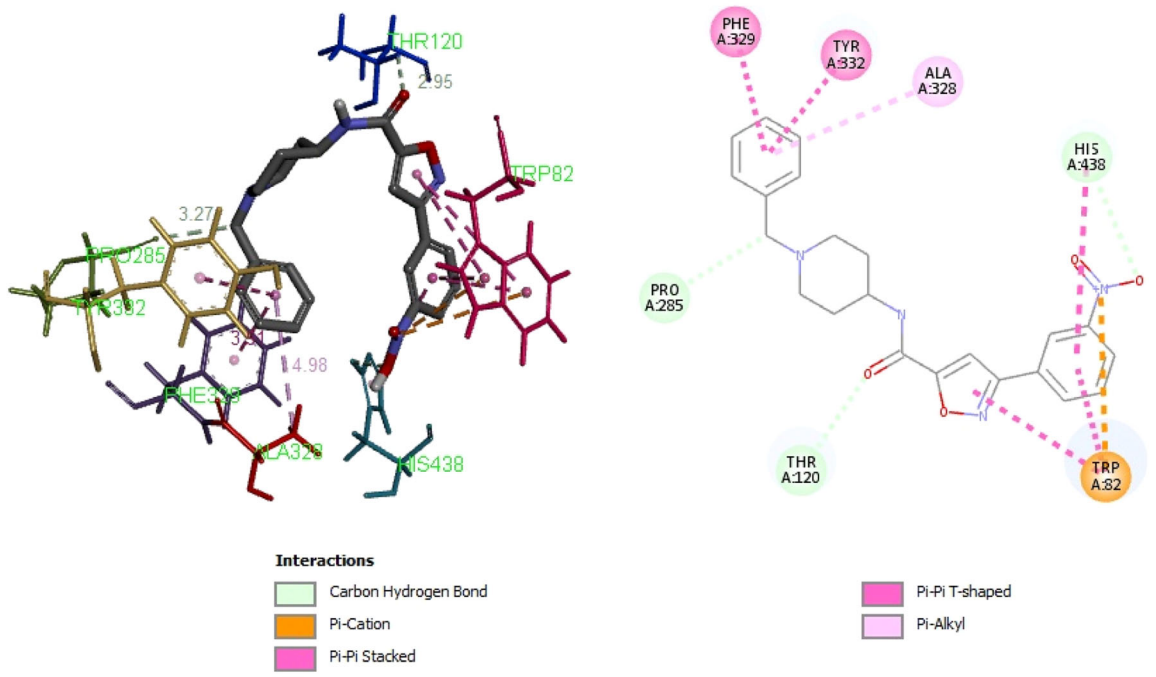

FIGURE 7 Docking of compound **4e** into the binding pocket of the 1P0P

with Asp72. Isoxazole and aryl ring enhanced energy minimization in the active site by forming π–donor hydrogen bonds with Tyr121 and Phe288, respectively.

The ligand was subjected to docking with the BuChE (1P0P), as demonstrated in Figure 7. Affinity values of the poses of the docked ligand ranged from −10.8 to −10.0 kcal/mol as a minimum. Similar to 1EVE active site interactions, nitroaryl moiety was fixed through H-bond and π stacking interactions via His438 and Trp82. The terminal aryl ring was captured by Ala328, Tyr332, and Phe329 via π–π interactions, π–alkyl interactions, and carbon–hydrogen bonds. For this derivative in 1P0P, the carbon–hydrogen bond interactions were also observed between the aliphatic part of the compound and residues Thr120 and Pro285.

The minimum affinity values for the best-docked confirmation of **4e** in the BACE1 (2QP8) active site ranged from −10.5 to −8.7 kcal/mol, which is related to the three conventional hydrogen bonds with Asp289, Thr133, and Asn98, and two carbon–hydrogen bonds with Asp93 and Tyr132 from the surrounding residues depicted in Figure 8. It was revealed that the specific binding characteristics in the BACE1 active site are associated with heteroatoms in amide linker, isoxazole ring, and nitroaryl moiety via hydrogen bonds.

Taken together, the enzymes' inhibition results and molecular interaction studies clearly suggested that the nitro group on the aryl ring played a crucial role to attach strongly into the active sites of 1EVE and 2QP8, which is responsible for influencing the inhibitory

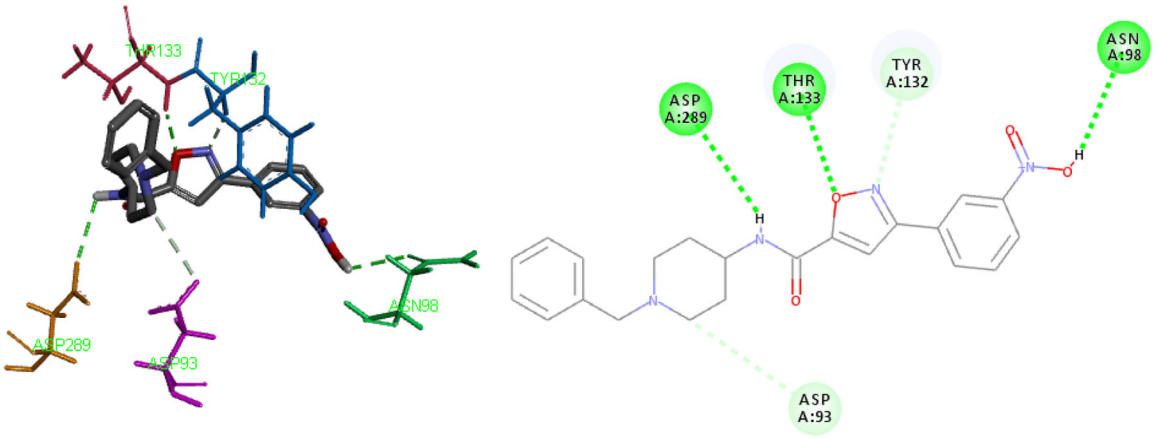

FIGURE 8 Docking of compound **4e** into the binding pocket of the 2QP8

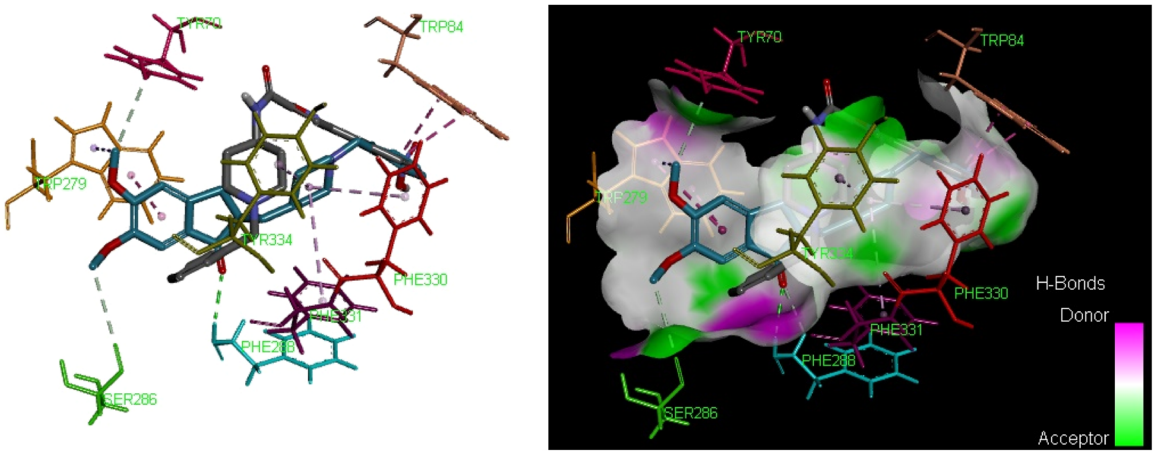

FIGURE 9 The representation of donepezil structure (in blue) and **4e** (in gray) in the 1EVE active site

activity, providing valuable information for the design of efficient inhibitors.

The presence of a hydrophilic group like the aryl ring was accountable for the improvement of activity, particularly in the BuChE active site.[21] In addition, the nitrogen of amide linker and oxygen of nitro group are the biggest contributors in compound **4e**, which are involved in the binding of the ligand through the H-bond in 1EVE and 2QP8.

1EVE binding site interactions for both reference ligand and compound **4e** are concurrently figured out in Figure 9. Donepezil (blue ligand) well occupied the entire length of the AChE aromatic gorge and formed H-bond and aromatic stacking interactions. There are several key binding interactions for donepezil and compound **4e** in the active site via Tyr70, Trp84, Asp72, Glu199, and Phe288, which are identified by the binding models according to the interactions with the AChE active site.

3 | CONCLUSION

In this study, a novel series of *N*-(1-benzylpiperidin-4-yl)-5-arylisoxazole-3-carboxamides analogs were designed and synthesized as MTDLs. The in vitro results revealed that compound **4e** bearing a *meta*-nitro group connected to isoxazole moiety was the best AChEI (IC_{50} = 16.07 μM) and BuChEI (IC_{50} = 15.16 μM). The *para*-nitro-substituted analog **4f** showed a selective anti-AChE activity (IC_{50} = 23.63 μM), whereas the compound **4c** bearing *meta*-OMe group was found to be a selective BuChE inhibitor (IC_{50} = 47.46 μM). Moreover, the molecular docking analysis provided a reasonable mechanism for the structure–activity relationship (SAR) analysis against ChE enzymes. The in vitro kinetic assay of **4e** presented a mixed type of inhibition pattern against both AChE and BuChE. Also, compound **4e** depicted 24.3% BACE1 inhibition at 50 μM, confirmed by the fluorescence resonance energy transfer (FRET)-based assay. More important, compound **4e** showed 23.2% neuroprotection on neuronal cell lines at 50 μM. Meanwhile, the metal chelation potential of **4e** was also investigated and the complexation ratio of 1:1 for 4e–Fe^{2+} was observed. The obtained results proposed that the arylisoxazole-benzylpiperidine-based compounds could be considered in the field of MTDLs against AD.

4 | EXPERIMENTAL

4.1 | Chemistry

4.1.1 | General

Melting points were taken on a Kofler hot-stage apparatus and were uncorrected. The ^{1}H and ^{13}C NMR spectra were recorded on Bruker FT-500, using TMS as an internal standard. The IR spectra were obtained on a Nicolet Magna FTIR 550 spectrophotometer (in KBr). Mass spectra were determined on an Agilent Technology (HP) mass spectrometer operating at an ionization potential of 70 eV. The elemental analysis was performed with an Elementar Analysensystem GmbH VarioEL CHNS mode. All reagents and solvents were obtained from Merck and Aldrich and used without purification.

The InChI codes of the investigated compounds, together with some biological activity data, are provided as Supporting Information.

4.1.2 | General procedure for the synthesis of compound 2

Here, 5-arylisoxazole-3-carboxylic acid derivative **2** was exactly prepared according to our previous report.[17] For this purpose, the solution of sodium ethoxide was freshly prepared by the reaction of sodium (1 mol) in dry EtOH (250 ml) in an ice bath. Then, a mixture of diethyl oxalate (1 mol) and an appropriate acetophenone derivative (1 mol) was added dropwise to that solution. The reaction was stopped by the formation of a yellow pasty material, which was left

at room temperature for 15 h. Next, it was stirred at 80°C in a water bath for 90 min and the crude was treated with dilute sulfuric acid to adjust to pH 2, affording an oily product that was extracted using chloroform and washed by saturated $NaHCO_3$ solution and brine. The organic phase was dried over Na_2SO_4 and the solvent was removed under vacuum to give 2,4-dioxo-4-aryl butanoate derivative, which was purified by recrystallization from chloroform and hexane. Next, a mixture of hydroxylamine hydrochloride (0.23 mol) and 2,4-dioxo-4-aryl butanoate derivative prepared in the previous step (0.08 mol) in ethanol (220 ml) was refluxed for 3 h. After the completion of the reaction (checking by TLC), the mixture was poured on crushed ice, and the precipitate was extracted by dichloromethane and washed with water, NaOH solution (4%), and brine, respectively. The organic phase was dried over Na_2SO_4 and the solvent was removed under vacuum to afford ethyl 5-arylisoxazole-3-carboxylate derivative, which was then subjected to alkaline hydrolysis. In this respect, ethyl 5-arylisoxazole-3-carboxylate (1 mmol) was treated with KOH (3 mmol) in methanol (15 ml) under reflux conditions for 3 h. After the completion of the reaction (checking by TLC), the mixture was poured into the water and ice, and a white precipitated product was formed when the concentrated HCl was added dropwise.

4.1.3 | General procedure for the synthesis of compounds 4a–l

A mixture of 5-arylisoxazole-3-carboxylic acid derivative **2** (1 mmol), HOBT (1 mmol), and EDCI (1 mmol) were stirred in dry acetonitrile (5 ml) at room temperature for 1 h, and then 1-benzylpiperidin-4-amine (**3**) (1 mmol) was added to the mixture and the reaction was continued for 24–72 h. After completion of the reaction (checking by TLC), the solvent was evaporated under vacuum, the crude was extracted using chloroform, and washed with water, solutions of $NaHCO_3$ 10%, saturated NaCl, and citric acid 10%, respectively. After drying the organic phase over sodium sulfate, the solvent was removed and the solid product was recrystallized from ethyl acetate and petroleum ether.

N-*(1-Benzylpiperidin-4-yl)-5-phenylisoxazole-3-carboxamide (**4a**)*

Yield: 67%, m.p. = 239–245°C. IR (KBr): 3247, 2929, 1671, 1542, 1442 cm^{-1}. ^1H NMR (500 MHz, DMSO-d_6): 9.06 (bs, 1H, NH), 7.95–7.90 (m, 3H, H2, H4, H6), 7.62–7.40 (m, 8H, Ph, isoxazole, H3, H5), 4.39–4.37 (m, 1H, CH), 4.25 (s, 2H, CH_2), 3.32–3.30 (m, 2H, CH_2), 3.08–3.06 (m, 2H, CH_2), 2.04–1.98 (m, 4H, CH_2). ^{13}C NMR (125 MHz, DMSO-d_6) (two isomers): 171.1, 170.3, 159.5, 159.4, 158.3, 156.9, 131.4, 131.1, 130.9, 129.4, 128.8, 126.3, 125.8, 125.7, 100.8, 99.9, 62.0, 50.5, 44.0, 30.8. Anal. calc. for $C_{22}H_{23}N_3O_2$: C, 73.11; H, 6.41; N, 11.63. Found: C, 73.30; H, 6.25; N, 11.45.

N-*(1-Benzylpiperidin-4-yl)-5-(*p*-tolyl)isoxazole-3-carboxamide (**4b**)*

Yield: 51%, m.p. greater than 250°C. IR (KBr): 3280, 2925, 2850, 1671, 1614, 1547 cm^{-1}. ^1H NMR (500 MHz, $CDCl_3$): 12.75 (s, 1H, NH), 7.64 (d, J = 8.0 Hz, 2H, H_2 H_6), 7.47–7.17 (m, 7H, Ph, H_3, H_5), 6.86 (s, 1H, isoxazole), 4.18 (s, 2H, CH_2), 3.56–3.53 (m, 1H, CH), 2.82–2.80 (m, 2H, CH_2), 2.55–2.52 (m, 2H, CH_2), 2.43–2.39 (m, 5H, CH_2, CH_3), 2.20–2.17 (m, 2H, CH_2). ^{13}C NMR (125 MHz, $CDCl_3$): 158.8, 158.5, 141.2, 133.4, 131.5, 130.3, 129.8, 129.4, 127.8, 125.8, 124.0, 98.3, 60.9, 51.3, 44.7, 28.6, 21.5. Anal. calc. for $C_{23}H_{25}N_3O_2$: C, 73.57; H, 6.71; N, 11.19. Found: C, 73.71; H, 6.56; N, 10.91.

N-*(1-Benzylpiperidin-4-yl)-5-(3-methoxyphenyl)isoxazole-3-carboxamide (**4c**)*

Yield: 53%, m.p. = 155–157°C. IR (KBr): 3322, 3090, 2928, 2853, 1648, 1610, 1575, 1547 cm^{-1}. ^1H NMR (500 MHz, $CDCl_3$): 7.40–7.28 (m, 8H, Ph, H2, H5, H6), 7.00 (dd, J = 7.4, 2.0 Hz, 1H, H4), 6.94 (s, 1H, isoxazole), 4.23–4.15 (m, 1H, CH), 4.25 (s, 2H, CH_2), 3.87 (s, 3H, OCH_3), 3.61–3.58 (m, 2H, CH_2), 2.96–2.93 (m, 2H, CH_2), 2.27–2.25 (m, 2H, CH_2), 2.06–2.02 (m, 2H, CH_2). ^{13}C NMR (125 MHz, $CDCl_3$) (two isomers): 171.5, 159.9, 159.8, 159.7, 146.9, 144.5, 131.4, 130.3, 129.6, 128.8, 127.7, 118.5, 116.3, 110.8, 62.0, 55.4, 51.1, 45.0, 31.2. Anal. calc. for $C_{23}H_{25}N_3O_3$: C, 70.57; H, 6.44; N, 10.73. Found: C, 70.74; H, 6.58; N, 10.58.

N-*(1-Benzylpiperidin-4-yl)-5-(4-nitrophenyl)isoxazole-3-carboxamide (**4d**)*

Yield: 70%, m.p. = 152–155°C. IR (KBr): 3308, 3084, 2940, 2848, 1658, 1606, 1548 cm^{-1}. ^1H NMR (500 MHz, DMSO-d_6): 8.61 (d, J = 8.0 Hz, 1H, NH), 7.48 (dd, J = 8.5, 2.0 Hz, 1H, H6), 7.44 (d, J = 2.0 Hz, 1H, H2), 7.34–7.23 (m, 6H, Ph, isoxazole), 7.10 (d, J = 8.5 Hz, 1H, H5), 3.85 (s, 3H, OCH_3), 3.82 (s, 3H, OCH_3), 3.81–3.79 (m, 1H, CH), 3.46 (s, 2H, CH_2), 2.82–2.80 (m, 2H, CH_2), 2.06–2.02 (m, 2H, CH_2), 1.76–1.74 (m, 2H, CH_2), 1.65–1.59 (m, 2H, CH_2). ^{13}C NMR (125 MHz, $CDCl_3$): 171.6, 159.3, 151.1, 149.3, 127.4, 128.4, 119.6, 119.3, 111.3, 108.5, 98.0, 96.1, 61.5, 56.1, 56.0, 52.0, 45.5, 30.5. Anal. calc. for $C_{24}H_{27}N_3O_4$: C, 68.39; H, 6.46; N, 9.97. Found: C, 68.59; H, 6.28; N, 10.21.

N-*(1-Benzylpiperidin-4-yl)-5-(3-nitrophenyl)isoxazole-3-carboxamide (**4e**)*

Yield: 62%, m.p. = 117–119°C. IR (KBr): 3383, 3082, 2930, 1675, 1528, 1449, 1348 cm^{-1}. ^1H NMR (500 MHz, $CDCl_3$): 12.71 (s, 1H, NH), 8.61 (s, 1H, H2), 8.32 (d, J = 8.0 Hz, 1H, H6), 8.11 (d, J = 8.0 Hz, 1H, H4), 7.74–7.64 (m, 3H, H5, Ph), 7.49–7.46 (m, 3H, Ph), 7.11 (s, 1H, isoxazole), 4.22–4.18 (m, 3H, CH, CH_2), 3.57–3.55 (m, 2H, CH_2), 2.86–2.79 (m, 2H, CH_2), 2.61–2.54 (m, 2H, CH_2), 2.21–2.18 (m, 2H, CH_2). ^{13}C NMR (125 MHz, $CDCl_3$): 168.9, 159.1, 158.0, 148.7, 132.9, 131.3, 130.7, 130.4, 129.3, 129.1, 128.2, 125.1, 120.8, 100.8, 61.4, 51.4, 45.3, 29.4. ^{13}C NMR (125 MHz, $CDCl_3$): Anal. calc. for $C_{22}H_{22}N_4O_4$: C, 65.01; H, 5.46; N, 13.78. Found: C, 64.87; H, 5.66; N, 13.54.

N-*(1-Benzylpiperidin-4-yl)-5-(4-nitrophenyl)isoxazole-3-carboxamide (**4f**)*

Yield: 62%, m.p. = 117–119°C. IR (KBr): 3241, 3071, 2950, 1676, 1607, 1560 cm^{-1}. ^1H NMR (500 MHz, $CDCl_3$): 8.35 (d, J = 8.2 Hz, 2H,

H2, H6), 7.99 (d, *J* = 8.2 Hz, 2H, H3, H5), 7.42–7.34 (m, 5H, Ph), 7.16 (s, 1H, isoxazole), 4.13–4.09 (m, 1H, CH), 3.87 (s, 2H, CH_2), 3.22–3.20 (m, 2H, CH_2), 2.67–2.52 (m, 4H, CH_2), 2.11–1.95 (m, 2H, CH_2). ^{13}C NMR (125 MHz, $CDCl_3$): 165.6, 161.5, 157.0, 147.0, 141.0, 131.3, 131.2, 129.4, 129.3, 126.7, 124.5, 101.8, 63.0, 52.5, 45.8, 30.5. Anal. calc. for $C_{22}H_{22}N_4O_4$: C, 65.01; H, 5.46; N, 13.78. Found: C, 64.71; H, 5.27; N, 13.90.

N-*(1-Benzylpiperidin-4-yl)-5-(2-fluorophenyl)isoxazole-3-carboxamide (**4g**)*

Yield: 53%, m.p. = 222–224°C. IR (KBr): 3300, 2964, 2667, 1665, 1617, 1593, 1542 cm^{-1}. ^{1}H NMR (500 MHz, $CDCl_3$): 12.34 (s, 1H, NH), 7.89–7.86 (m, 1H, H6), 7.67–7.65 (m, 1H, H4), 7.45–7.41 (m, 5H, Ph), 7.24 (t, *J* = 8.0 Hz, 1H, H3), 7.16 (t, *J* = 8.0 Hz, 1H, H5), 7.07 (s, 1H, isoxazole), 4.52–4.41 (m, 1H, CH), 4.26 (s, 2H, CH_2), 3.57–3.55 (m, 2H, CH_2), 3.00–2.87 (m, 2H, CH_2), 2.55–2.48 (m, 2H, CH_2), 2.22–2.00 (m, 2H, CH_2). ^{13}C NMR (125 MHz, $CDCl_3$) (two isomers): 169.5, 165.8, 160.0 (d, J_{C-F} = 245.0 Hz), 158.7, 132.1 (d, J_{C-F} = 8.7 Hz), 131.5, 131.3, 130.2, 129.9, 128.6, 128.0, 127.4, 127.3, 127.0, 126.4, 125.7, 124.7, 116.3 (d, J_{C-F} = 21.2 Hz), 115.0 (d, J_{C-F} = 12.5 Hz), 102.9, 102.8, 60.7, 51.2, 44.7, 28.6. Anal. calc. for $C_{22}H_{22}FN_3O_2$: C, 69.64; H, 5.84; N, 11.07. Found: C, 69.48; H, 5.61; N, 10.85.

N-*(1-Benzylpiperidin-4-yl)-5-(4-fluorophenyl)isoxazole-3-carboxamide (**4h**)*

Yield: 65%, m.p. = 248–250°C. IR (KBr): 3235, 2931, 1671, 1616, 1545, 1503 cm^{-1}. ^{1}H NMR (500 MHz, $CDCl_3$): 7.79–7.76 (m, 1H, NH), 7.63–7.61 (m, 2H, H2, H6), 7.48–7.45 (m, 5H, Ph), 7.18 (t, *J* = 8.5 Hz, 2H, H3, H5), 6.87 (s, 1H, isoxazole), 4.18–4.14 (m, 3H, CH, CH_2), 3.55–3.52 (m, 2H, CH_2), 2.80–2.75 (m, 2H, CH_2), 2.56–2.51 (m, 2H, CH_2), 2.20–2.17 (m, 2H, CH_2). ^{13}C NMR (125 MHz, $CDCl_3$) (two isomers): 176.4, 160.4 (d, J_{C-F} = 245.6 Hz), 163.2, 162.1, 157.5, 149.6, 145.5, 144.8, 136.2, 131.7, 131.2, 129.1, 128.1, 126.2, 123.9, 117.1, 115.0, 106.8, 101.4, 60.5, 52.0, 40.1, 30.4. Anal. calc. for $C_{22}H_{22}FN_3O_2$: C, 69.64; H, 5.84; N, 11.07. Found: C, 69.77; H, 5.64; N, 11.22.

N-*(1-Benzylpiperidin-4-yl)-5-(2-chlorophenyl)isoxazole-3-carboxamide (**4i**)*

Yield: 55%, m.p. = 158–160°C. IR (KBr): 3245, 3093, 2930, 1671, 1612, 1540 cm^{-1}. ^{1}H NMR (500 MHz, $CDCl_3$): 7.94–7.92 (m, 1H, NH), 7.64–7.62 (m, 2H, H3, H6), 7.48–7.40 (m, 6H, Ph, H4), 7.33 (s, 1H, isoxazole), 7.19 (m, 1H, H5), 4.19–4.16 (m, 2H, CH_2), 3.56–3.54 (m, 1H, CH), 2.84–2.78 (m, 2H, CH_2), 2.59–2.51 (m, 2H, CH_2), 2.20–2.18 (m, 2H, CH_2), 1.73–1.69 (m, 2H, CH_2). ^{13}C NMR (125 MHz, DMSO-d_6): 167.9, 159.1, 156.6, 144.2, 132.5, 131.7, 131.5, 131.0, 131.0, 130.0, 129.5, 128.0, 124.7, 104.7, 62.1, 50.1, 40.5, 30.2. Anal. calc. for $C_{22}H_{22}ClN_3O_2$: C, 66.75; H, 5.60; N, 10.61. Found: C, 66.52; H, 5.75; N, 10.78.

N-*(1-Benzylpiperidin-4-yl)-5-(4-chlorophenyl)isoxazole-3-carboxamide (**4j**)*

Yield: 62%, m.p. greater than 250°C. IR (KBr): 3270, 2950, 1671, 1604, 1544, 1489, 1443 cm^{-1}. ^{1}H NMR (500 MHz, DMSO-d_6): 9.10 (d, *J* = 5.8 Hz, 1H, NH), 7.94 (d, *J* = 8.1 Hz, 2H, H2, H6), 7.62–7.61 (m, 3H, H3, H5, Ph), 7.45–7.45 (m, 5H, Ph, isoxazole), 4.25 (s, 2H, CH_2), 4.13–4.11 (m, 1H, CH_2), 3.21–3.20 (m, 2H, CH_2), 3.07–3.05 (m, 2H, CH_2), 2.00–1.98 (m, 2H, CH_2), 1.34–1.26 (m, 2H, CH_2). ^{13}C NMR (125 MHz, DMSO-d_6) (two isomers): 169.2, 167.0, 166.8, 159.6, 158.1, 135.5, 131.7, 131.6, 131.5, 129.5, 128.8, 127.6, 125.1, 100.5, 58.9, 50.4, 44.7, 38.1. Anal. calc. for $C_{22}H_{22}ClN_3O_2$: C, 66.75; H, 5.60; N, 10.61. Found: C, 66.59; H, 5.42; N, 10.48.

N-*(1-Benzylpiperidin-4-yl)-5-(2,4-dichlorophenyl)isoxazole-3-carboxamide (**4k**)*

Yield: 62%, m.p. = 170–172°C. IR (KBr): 3290, 3078, 3029, 2927, 2800, 1657, 1597, 1545 cm^{-1}. ^{1}H NMR (500 MHz, DMSO-d_6): 8.74 (d, *J* = 7.5 Hz, 1H, NH), 7.95 (d, *J* = 8.5 Hz, 1H, H6), 8.94 (d, *J* = 2.0 Hz, 1H, H3), 7.64 (dd, *J* = 8.5, 2.0 Hz, 1H, H5), 7.34–7.25 (m, 6H, Ph, isoxazole). ^{13}C NMR (125 MHz, $CDCl_3$): 171.8, 166.7, 159.1, 157.9, 143.0, 137.0, 131.9, 130.9, 130.0, 129.3, 128.4, 127.7, 124.2, 104.1, 62.8, 52.0, 46.6, 31.6. Anal. calc. for $C_{22}H_{21}Cl_2N_3O_2$: C, 61.40; H, 4.92; N, 9.76. Found: C, 61.65; H, 5.23; N, 9.58.

N-*(1-Benzylpiperidin-4-yl)-5-(4-bromophenyl)isoxazole-3-carboxamide (**4l**)*

Yield: 67%, m.p. = 158–160°C. IR (KBr): 3335, 2944, 2802, 1654, 1605, 1541 cm^{-1}. ^{1}H NMR (500 MHz, DMSO-d_6): 8.70 (d, *J* = 6.5 Hz, 1H, NH), 7.87 (d, *J* = 8.5 Hz, 2H, H2, H6), 7.76 (d, *J* = 8.5 Hz, 2H, H3, H5), 7.39 (s, 1H, isoxazole), 7.34–7.27 (m, 5H, Ph), 3.90–3.70 (m, 1H, CH), 3.52 (s, 2H, CH_2), 2.88–2.85 (m, 2H, CH_2), 2.60–2.55 (m, 2H, CH_2), 1.77–1.64 (m, 4H, CH_2). ^{13}C NMR (125 MHz, DMSO-d_6): 170.5, 159.3, 158.0, 143.2, 134.1, 132.4, 129.2, 128.3, 127.3, 125.6, 125.2, 99.5, 62.8, 52.0, 46.7, 31.7. Anal. calc. for $C_{22}H_{22}BrN_3O_2$: C, 60.01; H, 5.04; N, 9.54. Found: C, 60.15; H, 4.81; N, 9.70.

4.2 | Biological activity

4.2.1 | Anticholinesterase activity

All enzymes and reagents required for the assay were obtained from Aldrich. The in vitro anticholinesterase activity of all synthesized compounds, **4a–l**, was assayed using modified Ellman's method using a 96-well plate reader (BioTek ELx808).[12,22] Initially, the stock solutions of compounds **4** were prepared by dissolving the test compound (1 mg) in dimethyl sulfoxide (DMSO; 1 ml), and then diluted solutions at final concentrations of 1, 10, 20, and 40 μg/ml were prepared using methanol. Each well contained 50 μl potassium phosphate buffer (KH_2PO_4/K_2HPO_4, 0.1 M, pH 8), 25 μl sample solution, and 25 μl enzyme (final concentration: 0.22 U/ml in buffer). Control experiments were also performed under the same conditions without enzyme. After incubation at room temperature for 15 min, 125 μL DTNB (3 mM in buffer) was added and the characterization of enzymatic reaction was spectrometrically performed at 405 nm, followed by the addition of substrate (ATCI 3 mM in water) after 5–10 min. The IC_{50} values were determined graphically from

inhibition curves (log inhibitor concentration vs. percent of inhibition). Also, the same method was used for the BuChE inhibition assay.

4.2.2 | Kinetic studies

The kinetic study for the inhibition of AChE and BuChE by compound **4e** was carried out according to Ellman's method used for the inhibition assay with four different concentrations of inhibitors.[22] For the kinetic study of AChE, compound **4e** was used at the concentrations of 0, 7.39, 29.55, and 59.11 μM. The Lineweaver–Burk reciprocal plot was constructed by plotting 1/V against 1/[S] at variable concentrations of the substrate acetylthiocholine (187.5, 750, 1500, 3000 μM). The inhibition constant K_i was calculated by the plot of slopes versus the corresponding concentrations of the compound **4e**. The same method was performed for the kinetic study of BuChE using the same concentrations of compound **4e** and butyrylthiocholine.[12,23]

4.2.3 | BACE1 enzymatic assay

A FRET-based BACE1 enzyme assay kit was used to evaluate the inhibitory activity of compound **4e** against BACE1. The kit was purchased from Invitrogen (former Pan Vera Corporation) and the evaluation procedure was conducted according to the manufacturer's instructions.[24–26] BACE1 (purified baculovirus-expressed enzyme) was diluted using buffer (50 mM sodium acetate, pH 4.5) to prepare a 3× working solution of 1 U/ml. The peptide substrate (RhEVNLDAEFK-Quencher) was also diluted in the same buffer to obtain the 3× stock solution. DMSO stock solutions were diluted with buffer to give 3× solution of test samples at different concentrations. The 3× solution of the BACE1 enzyme (10 μl) and each inhibitor sample (10 μl) were placed in 96-well plates and gently mixed. The substrate 3× solution (10 μl) was then added to this mixture in each well to initiate the reaction at the final reaction volume of 30 μl. The reaction mixtures were incubated at 25°C for 90 min in the dark, and then the reaction was stopped by adding 10 μl of 2.5 mM sodium acetate. Fluorescence was monitored at 544 nm (excitation wavelength) and 590 nm (emission wavelength). OM99-2 was used as the reference drug, the IC_{50} value was calculated with CurveExpert software version 1.34 for Windows, and each experiment was repeated three to five times.

4.2.4 | Neuroprotection effect against Aβ-induced damage

The neuroprotective effect of compound **4e** to protect neuronal PC12 cells against damage induced by $A\beta_{25-35}$ was examined according to our previous report.[27] The MTT reduction assay was used to evaluate the neuroprotectivity of compound **4e** on neuronal PC12 cell damage induced by $A\beta_{25-35}$. The cells were grown in monolayer culture on collagen-coated plates at 37°C in a humidified atmosphere of 5% CO_2. Neuronal PC12 cells were plated at a density of 5×10^5 cells/well on 96-well plates. The cells were preincubated with compound **10h** for 3 h before human $A\beta_{25-35}$ (final concentration of 5 μM) was added. After 24 h, 90 μl medium was taken out and 20 μl of MTT (0.5 mg/ml dissolved in RPMI containing phenol red) was added and incubated for an additional 2 h at 37°C. The absorbance (A570 nm) was measured using a Bio-Rad microplate reader (Model 680; Bio-Rad). The details were reported in our previous work.

4.2.5 | Metal chelating activity

To study the metal-binding ability of compound **4e**, a mixture of methanolic solutions of the compound (1 ml) and the related metal (1 ml; prepared from $FeSO_4$, $ZnCl_2$, and $CuCl_2{\cdot}2H_2O$) with the same final concentrations (20 μM) in a quartz cuvette was incubated at room temperature for 30 min. Then, the absorption spectra were recorded in the range of 200–600 nm. The stoichiometry of complex **4e**–Fe^{2+} was also studied using the molar ratio method.[28] The concentration of compound **4e** was 20 μM and the final concentration of Fe^{2+} ranged from 0 to 40 μM with 4-μM intervals at 258.7 nm. The plot was obtained by the corresponding absorption versus the mole fraction of Fe^{2+} toward ligand **4e**.

4.3 | Molecular docking study

To figure out the binding modes of the most active compound **4e**, the docking simulation was performed to target the crystal structures of AChE, BuChE, and BACE1. The crystal structures of 1EVE, 1P0P, and 2QP8 were retrieved from the PDB and were docked using the AutoDock software.[17] Flexible ligand dockings were accomplished for the selected compound. The best positions of the selected compound in each target protein were chosen by analyzing the interactions between the enzymes and inhibitor. The best scoring positions, as achieved by the docking score, were then selected and visualized using Discovery Studio Client 2017.[17]

ACKNOWLEDGMENT

This study was financially supported by Tehran University of Medical Sciences with project No. 99-3-104-49878.

CONFLICT OF INTERESTS

The authors declare that there are no conflicts of interests.

ORCID

Aida Iraji http://orcid.org/0000-0002-8442-2205
S. Sara Mirfazli http://orcid.org/0000-0001-7171-683X
Tahmineh Akbarzadeh http://orcid.org/0000-0002-0212-7297

REFERENCES

[1] G. Amadoro, V. Latina, V. Corsetti, P. Calissano, *Biochim. Biophys. Acta, Mol. Basis Dis.* **2020**, *1866*, 165584.
[2] P.-P. Liu, Y. Xie, X.-Y. Meng, J.-S. Kang, *Signal Transduct. Target. Ther.* **2019**, *4*, 29.
[3] A. Iraji, M. Khoshneviszadeh, O. Firuzi, M. Khoshneviszadeh, N. Edraki, *Bioorg. Chem.* **2020**, *97*, 103649.
[4] P. J. Flannery, E. Trushina, *Mol. Cell. Neurosci.* **2019**, *98*, 109.
[5] M. Zhu, X. Wang, L. Sun, M. Schultzberg, E. Hjorth, *Ther. Adv. Neurol. Disord.* **2018**, *11*, 1756286418791107.
[6] S. G. F. Dá Mesquita, *Ph.D. Thesis*, Universidade do Minho (Portugal) **2015**.
[7] T. Ozben, S. Ozben, *Clin. Biochem.* **2019**, *72*, 87.
[8] A. C. Kim, S. Lim, Y. K. Kim, *Int. J. Mol. Sci.* **2018**, *19*, 128.
[9] G. I. Grasso, F. Bellia, G. Arena, C. Satriano, G. Vecchio, E. Rizzarelli, *Eur. J. Med. Chem.* **2017**, *135*, 447.
[10] M. G. Savelieff, S. Lee, Y. Liu, M. H. Lim, *ACS Chem. Biol.* **2013**, *8*, 856.
[11] D. P. Veitch, M. W. Weiner, P. S. Aisen, L. A. Beckett, N. J. Cairns, R. C. Green, D. Harvey, C. R. Jack, W. Jagust, J. C. Morris, R. C. Petersen, A. J. Saykin, L. M. Shaw, A. W. Toga, J. Q. Trojanowski, *Alzheimers Dement.* **2019**, *15*, 106.
[12] F. Vafadarnejad, M. Mahdavi, E. Karimpour-Razkenari, N. Edraki, B. Sameem, M. Khanavi, M. Saeedi, T. Akbarzadeh, *Bioorg. Chem.* **2018**, *77*, 311.
[13] F. Vafadarnejad, E. Karimpour-Razkenari, B. Sameem, M. Saeedi, O. Firuzi, N. Edraki, M. Mahdavi, T. Akbarzadeh, *Bioorg. Chem.* **2019**, *92*, 103192.
[14] Z. Haghighijoo, S. Akrami, M. Saeedi, A. Zonouzi, A. Iraji, B. Larijani, H. Fakherzadeh, F. Sharifi, S. M. Arzaghi, M. Mahdavi, N. Edraki, *Bioorg. Chem.* **2020**, *103*, 104146.
[15] Y.-J. Wu, J. Guernon, F. Yang, L. Snyder, J. Shi, A. McClure, R. Rajamani, H. Park, A. Ng, H. Lewis, C. Chang, D. Camac, J. H. Toyn, M. K. Ahlijanian, C. F. Albright, J. E. Macor, L. A. Thompson, *ACS Med. Chem. Lett.* **2016**, *7*, 271.
[16] M. Saeedi, D. Mohtadi-Haghighi, S. S. Mirfazli, M. Mahdavi, R. Hariri, H. Lotfian, N. Edraki, A. Iraji, O. Firuzi, T. Akbarzadeh, *Chem. Biodivers.* **2019**, *16*, e1800433.
[17] M. Saeedi, A. Rastegari, R. Hariri, S. S. Mirfazli, M. Mahdavi, N. Edraki, O. Firuzi, T. Akbarzadeh, *Chem. Biodivers.* **2020**, *17*, e1900746.
[18] M. Koufaki, A. Tsatsaroni, X. Alexi, H. Guerrand, S. Zerva, M. N. Alexis, *Bioorg. Med. Chem.* **2011**, *19*, 4841.
[19] N. Agrawal, P. Mishra, *Med. Chem. Res.* **2018**, *27*, 1309.
[20] A. Iraji, O. Firuzi, M. Khoshneviszadeh, M. Tavakkoli, M. Mahdavi, H. Nadri, N. Edraki, R. Miri, *Eur. J. Med. Chem.* **2017**, *141*, 690.
[21] I. Daoud, N. Melkemi, T. Salah, S. Ghalem, *Comput. Biol. Chem.* **2018**, *74*, 304.
[22] G. L. Ellman, K. D. Courtney, V. Andres Jr., R. M. Featherstone, *Biochem. Pharmacol.* **1961**, *7*, 88.
[23] Z. Najafi, M. Saeedi, M. Mahdavi, R. Sabourian, M. Khanavi, M. B. Tehrani, F. H. Moghadam, N. Edraki, E. Karimpor-Razkenari, M. Sharifzadeh, *Bioorg. Chem.* **2016**, *67*, 84.
[24] A. Iraji, O. Firuzi, M. Khoshneviszadeh, H. Nadri, N. Edraki, R. Miri, *Bioorg. Chem.* **2018**, *77*, 223.
[25] S. Azimi, A. Zonouzi, O. Firuzi, A. Iraji, M. Saeedi, M. Mahdavi, N. Edraki, *J. Med. Chem.* **2017**, *138*, 729.
[26] N. Edraki, O. Firuzi, Y. Fatahi, M. Mahdavi, M. Asadi, S. Emami, K. Divsalar, R. Miri, A. Iraji, M. Khoshneviszadeh, L. Firoozpour, A. Shafiee, A. Foroumadi, *Arch. Pharm.* **2015**, *348*, 330.
[27] M. Yazdani, N. Edraki, R. Badri, M. Khoshneviszadeh, A. Iraji, O. Firuzi, *Bioorg. Chem.* **2019**, *84*, 363.
[28] M. Karamać, *Int. J. Mol. Sci.* **2009**, *10*, 5485.

SUPPORTING INFORMATION

Additional supporting information may be found online in the supporting information tab for this article.

How to cite this article: Saeedi M, Felegari P, Iraji A, et al. Novel *N*-benzylpiperidine derivatives of 5-arylisoxazole-3-carboxamides as anti-Alzheimer's agents. *Arch Pharm.* 2020;e2000258. https://doi.org/10.1002/ardp.202000258